PHOTOGRAPHS OF PARTICLES FROM AN AEROBEE ROCKET AT 130 - 204 KM ALTITUDE†

by

R. Tousey, M. J. Koomen, R. E. McCullough and R. T. Seal
E. O. Hulburt Center for Space Research*
U. S. Naval Research Laboratory, Washington, D. C., 20390

Talk presented at

Symposium on Meteor Orbits and Dust
Astrophysical Observatory
Smithsonian Institution
Cambridge, Massachusetts
11 August 1965

(Revised - 3 September 1965)

†Work supported, in part, by the National Aeronautics and Space Administration

*Sponsored jointly by the Office of Naval Research and National Science Foundation.

(7140-PRR-16/65:RT:nrgw)

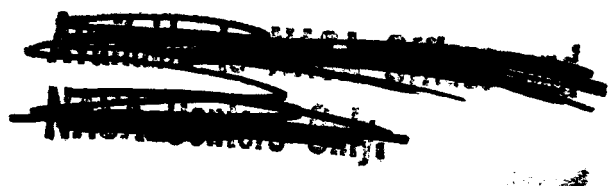

PHOTOGRAPHS OF PARTICLES FROM AN AEROBEE ROCKET AT 130 - 204 KM ALTITUDE[1]

R. Tousey, M. J. Koomen, R. E. McCullough, and R. T. Seal
E. O. Hulburt Center for Space Research*
U. S. Naval Research Laboratory, Washington, D. C., 20390

INTRODUCTION

A white light coronagraph, flown in an Aerobee-150 rocket from the White Sands Missile Range on June 28, 1963, was successful in photographing the sun's white light corona from 3.5 to 10 solar radii (R_s), something not previously accomplished without the aid of a total solar eclipse. The luminance of the white light corona was found to be approximately twice that recorded by experiments conducted during total eclipses (e.g., Blackwell, 1955). This doubled luminance was interpreted as evidence for dust within a few earth radii, which was illuminated by full sunlight in the rocket experiment, but was within the umbra or penumbra during an eclipse (Koomen, Purcell, Tousey, and Seal, 1964), (Tousey, 1965). A similar result has been found with the U. S. Naval Research Laboratory (NRL) photoelectric coronagraph on the second orbiting solar observatory (OSO-II) launched by the National Aeronautics and Space Administration (NASA). The coronal photographs were

---

[1] Work supported, in part, by the National Aeronautics and Space Administration.

*Sponsored jointly by the Office of Naval Research and National Science Foundation

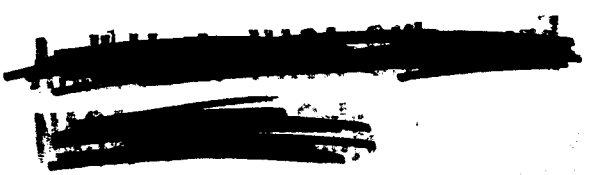

covered with artifacts of various types which resulted in much obscuration of the coronal features. Many were tracks of small particles, slowly crossing the field of view; some were close, and others far from the rocket. The altitudes at which the photographs were made ranged from 131 km to 204 km.

The instrument was a small Lyot coronagraph, with objective lens of focal length 30 cm and diameter 25 mm. An external occulter prevented direct sunlight from falling on the objective lens; sunlight diffracted from the occulter's edge was directed away from the lens by using the saw-toothed occulter design of Purcell and Koomen (1962). The residual stray light background level was about 10% of the coronal luminance for quiet solar conditions over the entire field of the instrument. The coronagraph was kept pointed at the sun with an accuracy of better than $\pm$ 1 arc min, but there was no control of rotation around the solar vector. A slow rotation of the focal plane was produced by the precession of the rocket, its rate varied during the precession cycle from zero to a maximum value of $\approx \pm 0.8^{o}$/sec. At the margin of the field, $R = 10\ R_s$, this was equivalent to about 2 arc min in yaw or pitch per second.

The coronagraph proved to be an excellent camera for photographing tiny particles in space. However a requirement for photographing them is that they cross the field of view with a rather small angular velocity, that is, that they be moving at very nearly the same velocity as the rocket, or else be far

away and very bright. This ruled out detecting small particles in geocentric orbits.

The reason that the coronagraph was able to photograph small particles is that they shone so brightly by scattered sunlight, because of the Mie Effect. From the inner to the outer edge of the field the scattering angles ranged from 1^{o} to 2.5^{o}. The theory of Mie shows that the forward-scattered intensity within this range of angles is enhanced over the intensity at other angles by a very large factor; for $1\ \mu$ diameter dielectric spheres of refractive index $= 1.33$ the factor is $\approx 10^{3}$, and for $10\ \mu$ spheres, $\approx 10^{5}$.

In the 23 exposures made during flight, reproduced in Fig. 1, many particle trails were photographed. Some of these were close by, as evidenced by their unsharp, and often very broad trails; others were far away, since their tracks were in perfect focus.

The question is, did these objects come from the rocket, or were they a small sample of natural objects in space? At first thought, one would suppose that they must have come from the rocket, since then they would have almost exactly its velocity, as required to produce the trails. There is, however, another possibility that is difficult to rule out. Although meteorites at these altitudes would in general be moving much too fast to photograph, there should be a few particles of natural origin having velocities very close to that of the rocket.

Particle tracks were recorded by Newkirk and Bohlin (1965) with their similar but larger balloon-borne coronagraph, flown on September 10, 1960. These particles, however, were shown to have originated from some Styrofoam insulation, since on a flight in 1965, when this material was not used, almost no trails were present. Moreover, these particles must have been very large, since the balloon reached only 30 km altitude. Here the sky luminance is still sufficient to produce a background which would swamp the trails of faint particles.

Explanation of the pictures

The photographs of Fig. 1 contain various features that must be explained in order to interpret the particle tracks. The separate exposures are arranged in sequence, but each picture is oriented with solar north at the top and east to the left. The external occulter and the arm supporting it cast a conspicuous shadow. This was very diffuse, because the instrument was focussed for infinity and the occulter was only 20 inches from the objective lens. The occulter therefore gave rise to a strong vignetting action. This can be seen from the last picture in Fig. 1, which is an exposure made with a uniform field in the laboratory. It happened that the vignetting function and the radial brightness function of the corona just about neutralized each other. Therefore the background exposure, produced by the corona, was approximately uniform in density over the entire field. The individual exposures ranged from 1.1 to 55.8 sec, causing their densities to differ widely. In the reproduction they were printed to appear as nearly alike as possible.

Of the various artifacts present, an array of permanent bright spots is conspicuous on each exposure. These spots were fixed in position from exposure to exposure, and are explained as being caused by particles loosened from the interior of the instrument and deposited on a lens surface during launch. There is a bright patch at the right edge of the occulter shadow, which gradually became less intense, until it was nearly absent in the last exposure. This was caused by a slight mispointing of the biaxial pointing control, which allowed a little of the light diffracted from the edge of the occulter to reach the objective lens. Also present are faint scratches on the film, produced during transport; these are the very sharp, parallel straight lines that are visible in the shortest exposures. The great lune in Exposures 3 and 4 is a double exposure, caused by failure to transport the film far enough to separate the frames completely.

The amount of rotation, caused by the rocket precession is shown for each exposure by the arrow at the left edge of the frame. Absence of the arrow indicates negligible rotation. Also shown is the mean position of the center of the shadow of the occulter support; this position rotates gradually in correspondence with the precession cycle of the rocket, as do the permanent specks on the optical surfaces.

Particle tracks.

The tracks of more than two dozen fairly well established particles are indicated in Fig. 1 by the letters a - z. They vary from extremely sharp tracks, such as x, to great blobs of light like f, produced by a particle

within a foot or so of the lens. A preliminary analysis of some of these tracks has been attempted.

The distance of each particle was established from the track width, assuming that the particle was small enough to be considered as a point source. The calculated relation between track width and particle distance, confirmed by laboratory measurements, is show in Fig. 2. The optical system was quite well corrected, and the image of a true point source at infinity, as registered on Eastman Kodak Spectroscopic 1-D, the emulsion employed, measured a minimum of 0.02 mm diameter, for a low density exposure. Because of the vignetting, out of focus images of points were actually crescent-like; for close particles this produced trails with a sharp inner edge like the unlabelled streak in Exposure 15. One difficulty in estimating distances from trail widths comes from the dependence of apparent width on the difference between the density of the trail and the density of the background, an effect produced by the nonuniform distribution of intensity across the out-of-focus image. Another, of course, lies in the assumption of a point source.

The angular velocity of particles crossing the field was established directly from the exposure time and the length of the trail, when both ends of the trail could be located. Another method employed undulations in the tracks, which were caused by hunting of the pointing control. These are extremely prominent in tracks x and w. Fig. 3 shows a portion of x greatly enlarged. Comparison of the undulation wavelength, exposure time, and trail length led to the

determination of the undulation frequency as one cycle per second. This was approximately the hunting frequency of the pointing control in both elevation and azimuth. The double amplitude of trail x was 30 - 35 μ, which corresponds to a tracking jitter of $\pm$ 10 arc sec; this was excellent stability for the biaxial pointing control system, which was the first of a new type, designed and constructed by a group at the University of Colorado under the direction of F. Wilshusen. Still another method of establishing the speed, when a trail ended on one exposure and began on the next was from the gap produced by the film transport time, which was about 0.2 sec.

A conspicuous characteristic of each trail is that there is very little change in density from the beginning to the end, even though the particle was changing distance rapidly. There is a simple explanation for this. For a given particle, the flux per unit area on the film, and hence the density, is given by

$$D = f(E \frac{1}{\dot{\theta}} \quad \frac{1}{w})$$

where E is the illumination produced at the objective by the particle at distance d, $\dot{\theta}$ is the angular speed of motion of the image, and w is the width of the trail. E varies as $\frac{1}{d^2}$, the "inverse square law", but $\dot{\theta}$ varies as $\frac{1}{d}$, and w does likewise provided d is large compared to the focal length of the lens. Therefore the track density is independent of the distance, for a particle of a given velocity, until the distance becomes so great that the track width is limited by the resolution of the film and optical system. Vignetting

makes no difference, because it simply changes the size of the out-of-focus image and consequent track width, but does not change the flux per unit area.

All of the trails are curved to a greater or less extent. In order to interpret the curve, it is necessary first to correct for rotation of the image plane during the exposure. This has been done in Fig. 4, which shows a composite pieced together from Exposures 19 - 23, and a diagram giving corrected paths for particles x, y, and w.

In Table I a summary is presented of the principal characteristics of the trails, to the extent that the analysis has been carried out. The velocity values refer to the component in the plane normal to the solar vector; they are relative to the rocket, and are based on the estimated distances and the measured angular velocity. The rocket velocity components were approximately 90 M/sec North, 23 M/sec East, and a vertical component ranging from 1.2 km/sec up at Exposure No. 1, to zero at peak, to 0.8 km/sec down at the end of Exposure No. 23.

It is obvious that the relative velocities of all the particles with respect to the rocket, ranging as they do from 0.1 to 1.5 M/sec, are very low compared to the actual rocket velocity, even at peak. This appears to be prima facie evidence that they originate from the rocket. There is, however, the alternative explanation that some, at least, are particles of natural origin. That they should all have almost exactly the same velocity as the rocket is simply a result of the selective action of the photographic coronagraph. For

faint particles, only those which move across the field with low angular velocity will be able to expose a trail, especially when the background is dense, as it is in the long exposures. If there is a large number density of small particles within the altitude range covered by the rocket, there should be a few within the velocity range that is photographable.

This selective action applies principally to the velocity component in the plane perpendicular to the solar vector, and is quite stringent. At peak, for example, it acts to select particles having a north velocity component of between 91 and 89 M/sec, and a vertical velocity of zero $\pm$ 1 M/sec. At Exposure No. 22, the vertical velocity must remain within 1 M/sec of the rapidly increasing free fall velocity which is near 700 M/sec, and the same north velocity component restriction still holds. For the velocity component along the solar vector, however, the selection effect is less stringent.

An estimate of particle size was made, based on the assumptions that the particles are spherical, have an index of 1.33, and non-metallic. This was done using the Mie Theory, as presented by Penndorf (1962), for λ = 5000 Å, and a scattering angle close to 0^{o}. It was also necessary to calibrate the coronagraph, so as to obtain approximate values of stellar magnitude for the various particles producing the trails. Laboratory calibrations using point sources of light, indicated that third magnitude stars were easily recorded in 2 sec, and fourth magnitude stars were photographable in 1 sec when they did not move in the field. An unexpected check was obtained in

flight from the third magnitude star μ-Geminorum, which happened to lie $1^{o}44'$ from the sun, well within the field of view. This was present in most of the pictures; it was a well exposed point, of diameter 0.02 mm in the 1 sec exposures, and was drawn out into a short arc in longer exposures where the rocket precession rotated the instrument. Figure 5 shows two exposures where the star trail is easily seen. The motion of the star also confirmed the analysis of the rocket precession, as derived from the magnetometer and the pointing control elevation angle.

The conclusion reached from the observed trails and the Mie Theory was that the particles photographed must have been in the range 10 μ diameter and larger. Particles smaller than 10 μ would have been too faint to photograph. Among the smallest and faintest is j, at a distance of at least 200 meters. Even farther is Particle No.1 of Fig. 6 whose trail width, 0.02 mm, indicates a distance of 500 M or more. According to the Mie Theory the luminous intensity increases with the fourth power of the diameter, approximately, for particles near 10 μ diameter. This means that only a small increase in diameter is required to account for the brighter trails. It appears that 20 or 30 μ may be the upper diameter limit of particles photographed. These particle sizes fall within the dimension limits of particles collected by Hemenway and Soberman (1965) and collaborators, from balloons and rockets following meteor showers. One may question the assumptions involved in applying the Mie Theory, but because the magnitude change with size is so very rapid, the shape and

optical constants should not be of too great importance in connection with the luminosity of the particle.

In connection with the possibility of a natural origin for these particles, it is useful to consider some details of the trails. In the first place, the particles seem to appear in puffs. Particles are few or absent in the first four exposures, then become prominent in the following exposures including the ninth, and are absent again in Exposures 11 and 12. Particles are again evident in Exposures 14 through 19, but have subsided markedly in Exposures 20 through 23. Although this sort of behavior might perhaps be expected of an outgassing rocket, it may also be characteristic of meteor showers.

For exposures earlier than No. 13, all trails were downward, indicating an ascending cloud of particles through which the rocket was ascending at a slightly greater velocity. Before peak, however, particles are present which were travelling upward faster than the rocket (Exposures 14 - 16). From about Exposure 20 on, the particles appear to be travelling up, as the rocket falls, and are a cloud not falling quite as fast as the rocket. In the north and south direction the particles for the most part, show a small velocity component relative to the rocket toward the south.

At first sight these small relative velocity effects may seem to be caused by drag by the atmosphere. However, at these altitudes the mean free path is very long. For example, at 204 km it is 220 M, and at 130 km it is 14 M. Under these conditions the drag should be quite small, even for 10 μ particles.

Moreover, one would certainly expect the drag effect to be altitude dependent; but there is no correlation between particle velocity relative to the rocket and altitude.

It is not at all easy to explain the behavior of particles x, y, and w by changes of speed produced by drag. Particle x is particularly puzzling. Its trail can be followed in each exposure, from 19 through 23, and is shown as a composite in Fig. 4. Its path is also shown replotted with the correction made for rotation of the instrument during exposure. This particle was far away, as evidenced by its sharp trail. It entered the field on the descent at 202 km, 2 km below peak, when the rocket velocity downward was about 70 M/sec, and stayed in the field for a full minute, until the rocket reached 174 km, where its velocity was 650 M/sec. First it fell faster than the rocket, but after 30 sec the rocket passed it by, and 30 sec later it left the field. In the N - S direction it entered with almost no relative velocity, for a time seemed to gain on the rocket, but left the field travelling south relative to the rocket. Critical inspection of the sharpness of the trail suggests that it was moving eastward faster than the rocket, since the trail is sharpest at the end of Exposure 23. Its distance, on entrance, was 100 M, and after 30 sec was 200 M.

Particle w entered late in Exposure 19, and appears faint because of the dense background of the 56-sec exposure. After correction it makes an angle of 26^{o} with the zenith. The trail of particle y is closely parallel

to particle w, though it entered earlier and left later. It is difficult to reconcile these two trails with possible atmospheric drag effects. If the south component of each is ascribed to drag, associated with the north rocket velocity, 90 M/sec, there would have to be a drag effect on the vertical component as well. But the constant character of the north component and the increasing vertical velocity would combine with the increasing drag at lower altitudes to cause these two trails to be strongly curved; since they probably are not of the same size they would not be expected to remain parallel.

Exposure 15 of Fig. 1 contains the largest collection of particles and is shown enlarged in Fig. 6. The rocket was near the top of its trajectory during this exposure and was approaching zero vertical velocity. This exposure shows many particles with relative horizontal motions, in a direction opposite to the horizontal travel of the rocket. However there are also particles with vertical motions which are now in the same direction as the rocket motion, that is, they are overtaking the rocket. In the direction toward the sun, two are approaching and others are receding. This situation cannot be explained by drag. In particular, consider particles 1, 2, m', and n (Fig. 6), with distances >500, >200, 200, and 200 M, respectively; no two paths are parallel, and their directions range through more than 90^{o}. Yet in this exposure these four particles lay with 2.5^{o} of each other. Without resorting to a collision process of some sort, it would be impossible to eject from the rocket four particles and have them reach this small, distant region with

velocities so far from parallel.

Amongst the particles which were very close to the coronagraph, there are many which show strongly curved paths. These may be caused by electrostatic effects. Another factor comes from the precession of the rocket, since the rocket nose, swinging around in a cone, would impart nonlinear transverse velocities to the coronagraph under certain conditions. However, strongly curved paths do not require that these particles originate from the rocket, since natural particles could equally well be strongly charged and be deflected when passing close by the rocket.

It is difficult to arrive at a really clearcut conclusion without making a calculation of the number density of photographable particles, based on known and estimated distributions at these altitudes. The best proof that they are natural particles is that many are far from the rocket and their behavior is not easy to explain on the basis of an origin from the rocket.

It is of interest that the date of the rocket flight, June 28, 1963, lies in the month when meteor counts are at a maximum, and is in the period of the Corvid, ß Taurid, and Draconid Showers, and only a few days after the Arietid Shower. Moreover, from May through November in the year 1963, according to McIntosh and Millman (1964), and Ellyett and Keay (1964), there was an unexpected increase in the meteor count, especially for small particles. Perhaps meteors entering more or less parallel to the earth's surface

produce, in the break-up process, enough fragments moving upward and reaching the 200 km level with relatively low velocities to account for the photographed trails.

References

Penndorf, R., 1962, J. Opt. Soc. Am. 52, 402.

Koomen, M. J., Purcell, J. D., Seal, R. T., Jr., and Tousey, R., 1964, J. Opt. Soc. Am. 54, 1409.

Blackwell, D. E., 1955, Mon. Not. Roy. Astron. Soc. 115, 44.

Tousey, R., 1965, Ann. d'Astrophys. 28, 600.

Purcell, J. D., and Koomen, M. J., 1962, J. Opt. Soc. Am. 52, 596; Sky and Telescope 24, 197.

Newkirk, G., Jr., and Bohlin, J. D., 1965, Ann. d'Astrophys. 28, 234, and private communication.

Ellyett, C. D., and Keay, C. S. L., 1964, Science 146, 1458.

McIntosh, B. A., and Millman, P. M., 1964, Science 146, 1457.

Hemenway, C. L., and Soberman, R. K., 1965, Symposium on Meteor Orbits and Dust, Smithsonian Inst., Astrophys. Observ., Cambridge, Mass.

TABLE 1

Preliminary analysis of particle trails; NE-3.129, June 28, 1963

Particle	Apparent Speed M/sec	Distance - Meters Initial	Final
a	0.1	4	20
b		very close	
c		16	21
d	0.35	9	50
e		4	3
f		very close	
g	0.1	9	9
h	0.2	20	70
i	0.2	1	70
j	1.0	200	200
k		4	5
k′		100	100
l		15	15
l′		15	15
l″		22	22
m	0.2	8	15
m′	0.52	200	200
n	0.16	200	200
o	0.45	26	26
o′	0.2	15	15
p	0.1	15	22
p′	0.35	100	100
q	0.2	35	55
r	0.2	100	44
s	0.2	100	44
t	0.7	30	90
u	0.1	13	21
v	0.03	1	9
w	0.24	50	50
x	0.1	100	200
y	0.5	100	100
z	0.2	15	27
1	> 1.55	> 500	> 500
2	> 0.20	> 200	> 200
3	0.11	30	30

LIST OF FIGURES

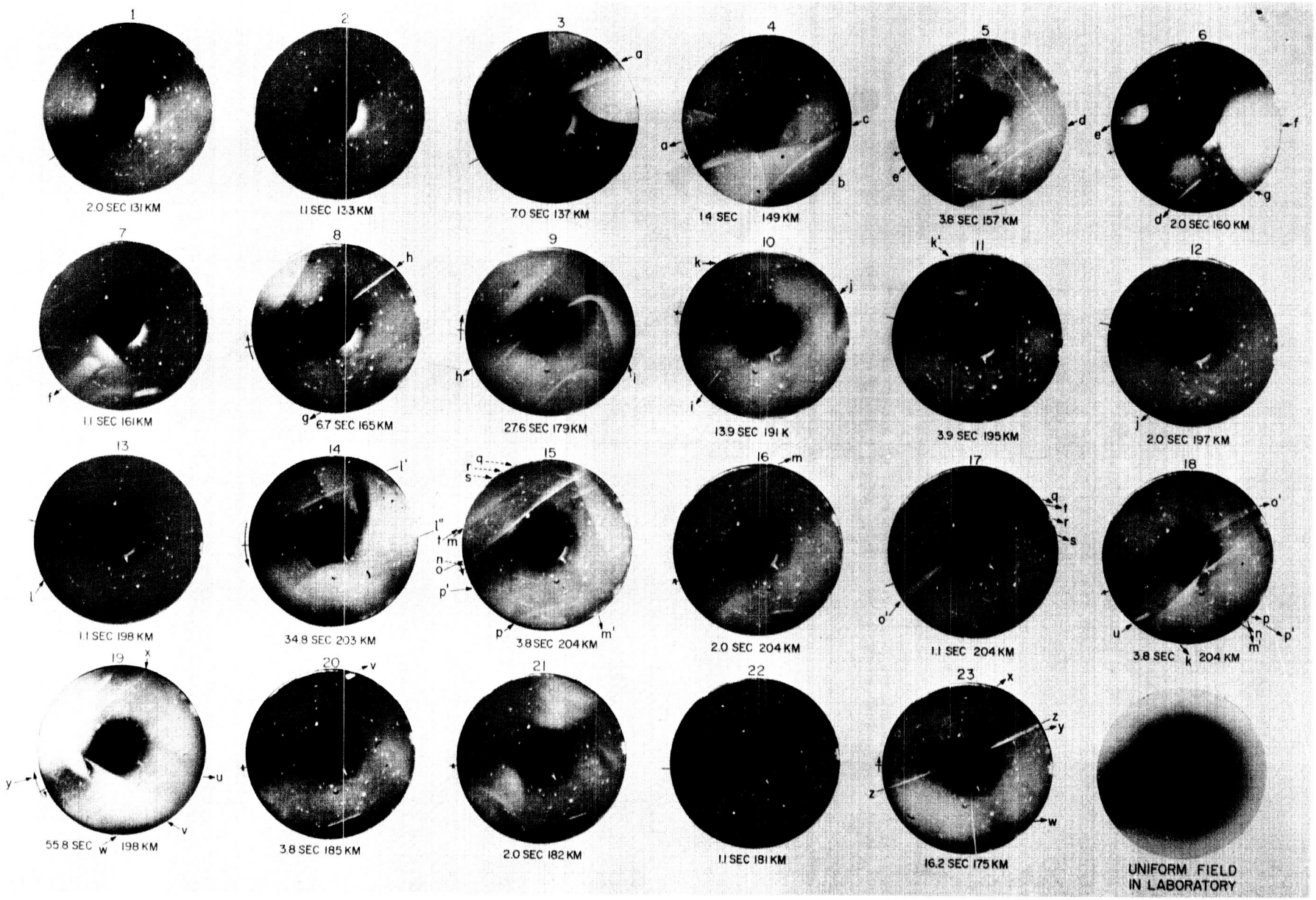
1
2.0 SEC 131 KM
2
1.1 SEC 133 KM
3
a
7.0 SEC 137 KM
4
a
c
b
1.4 SEC 149 KM
5
d
e
3.8 SEC 157 KM
6
e
f
g
d
2.0 SEC 160 KM
7
f
1.1 SEC 161 KM
8
h
g
6.7 SEC 165 KM
9
h
i
27.6 SEC 179 KM
10
k
j
i
13.9 SEC 191 K
11
k'
3.9 SEC 195 KM
12
j
2.0 SEC 197 KM
13
l
1.1 SEC 198 KM
14
l'
34.8 SEC 203 KM
15
q
r
s
l''
t
m
n
o
p'
p
m'
3.8 SEC 204 KM
16
m
2.0 SEC 204 KM
17
q
t
r
s
o'
1.1 SEC 204 KM
18
o'
u
p
n
m
p'
k
3.8 SEC 204 KM
19
x
y
u
v
w
55.8 SEC 198 KM
20
v
3.8 SEC 185 KM
21
2.0 SEC 182 KM
22
1.1 SEC 181 KM
23
x
z
y
z
w
16.2 SEC 175 KM
UNIFORM FIELD
IN LABORATORY

Fig. 1

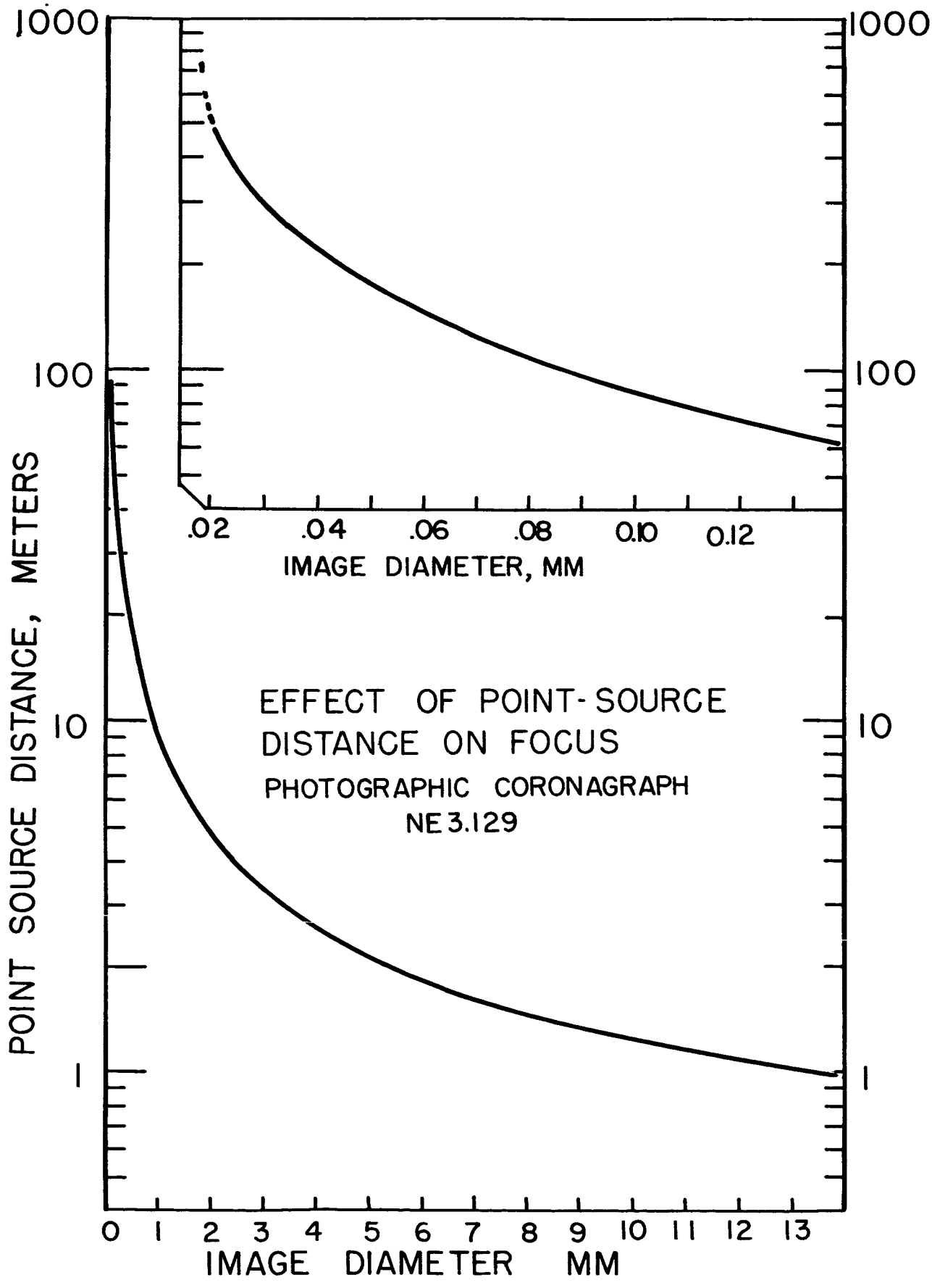
1000
100
10
1
POINT SOURCE DISTANCE, METERS
.02
.04
.06
.08
0.10
0.12
IMAGE DIAMETER, MM
EFFECT OF POINT-SOURCE
DISTANCE ON FOCUS
PHOTOGRAPHIC CORONAGRAPH
NE 3.129
0 1 2 3 4 5 6 7 8 9 10 11 12 13
IMAGE DIAMETER MM

Fig. 2

Fig 3

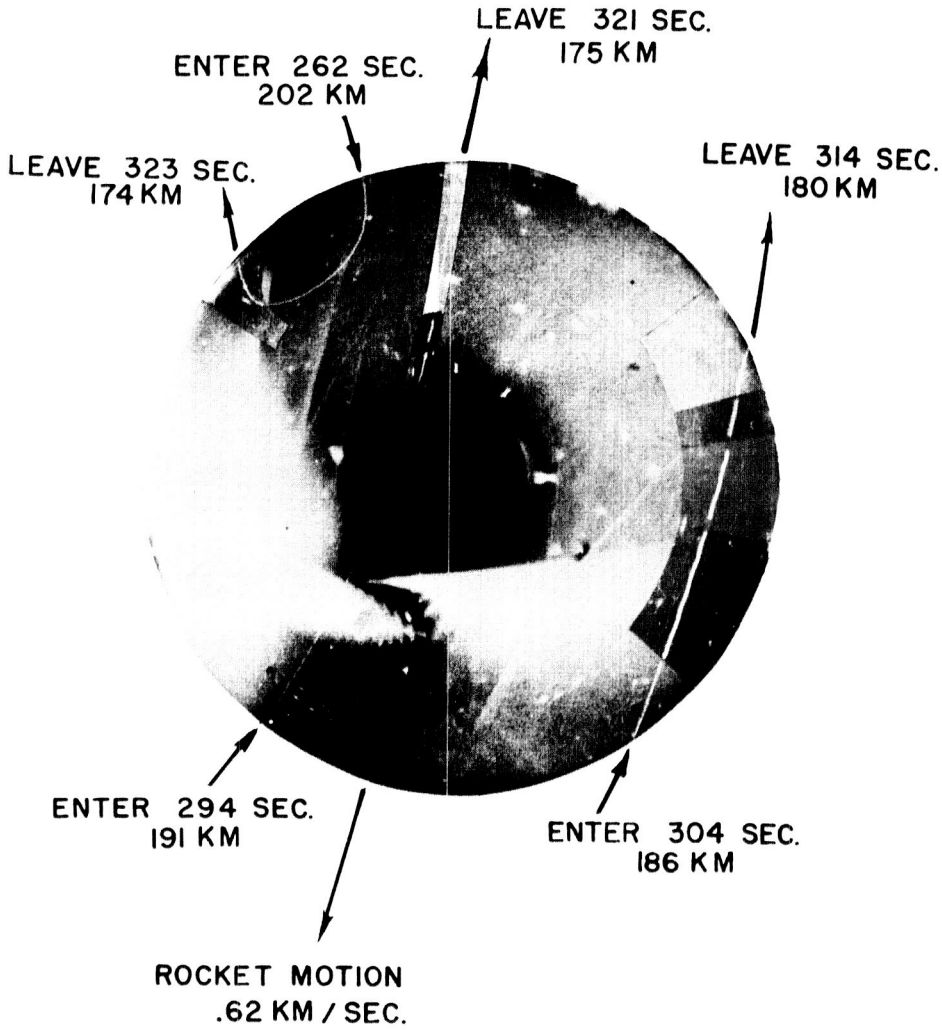

COMPOSITE OF EXPOSURES
19, 20, 21, 22, 23

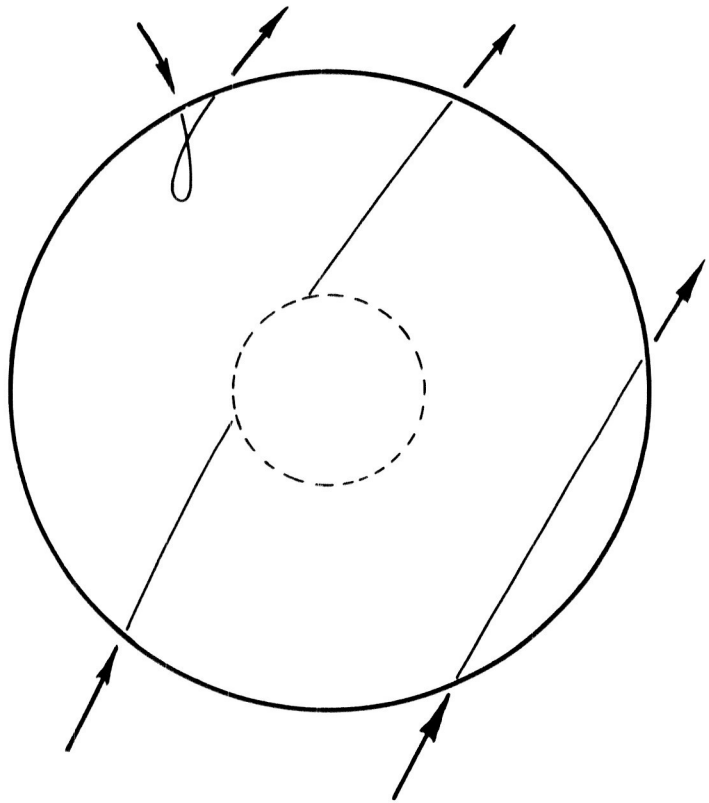

PARTICLE TRACKS CORRECTED
FOR ROTATION OF FOCAL PLANE

Fig. 4

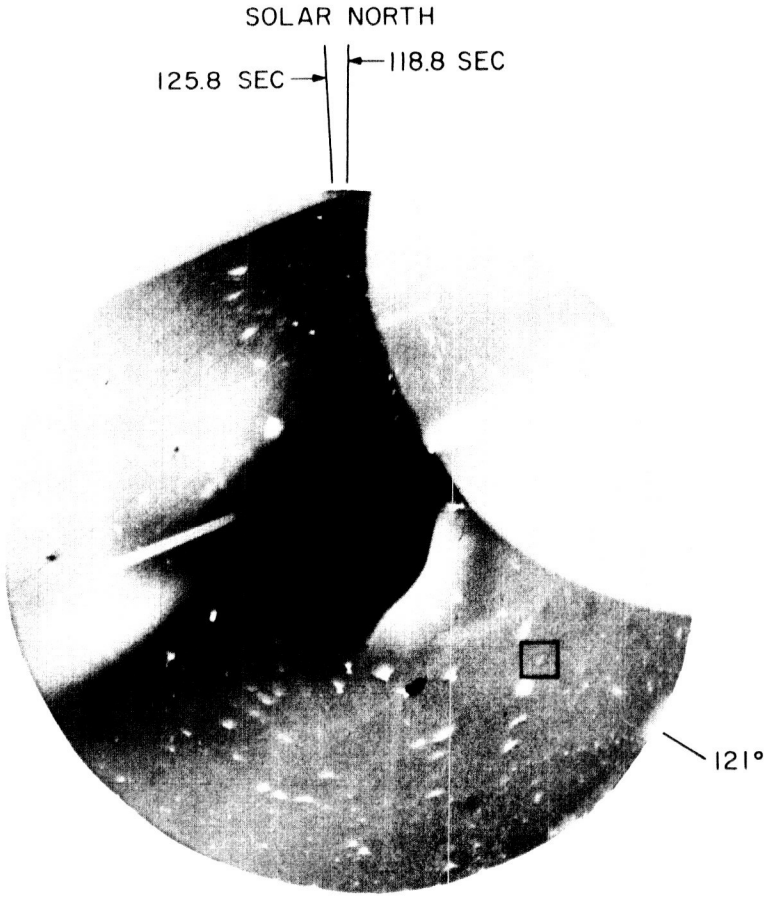

FRAME #3, 7.0 SEC, 137 KM

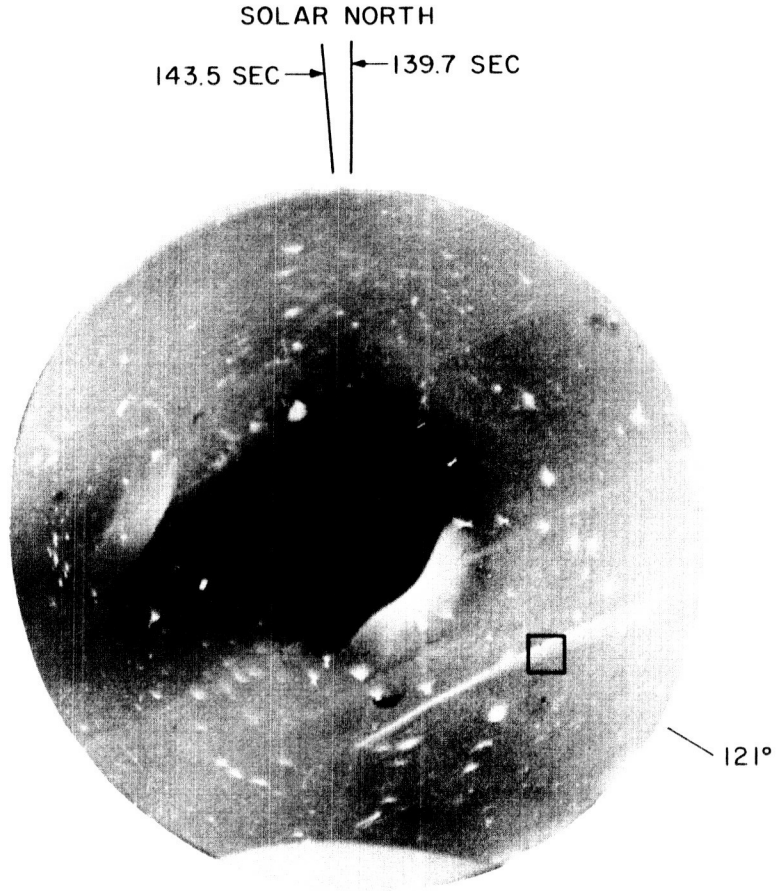

FRAME #5, 3.8 SEC, 160 KM

Fig. 5

μ - GEMINORUM, Mag. 2.86

AEROBEE NE 3.129 (CORONAGRAPH) 28 JUNE 1963

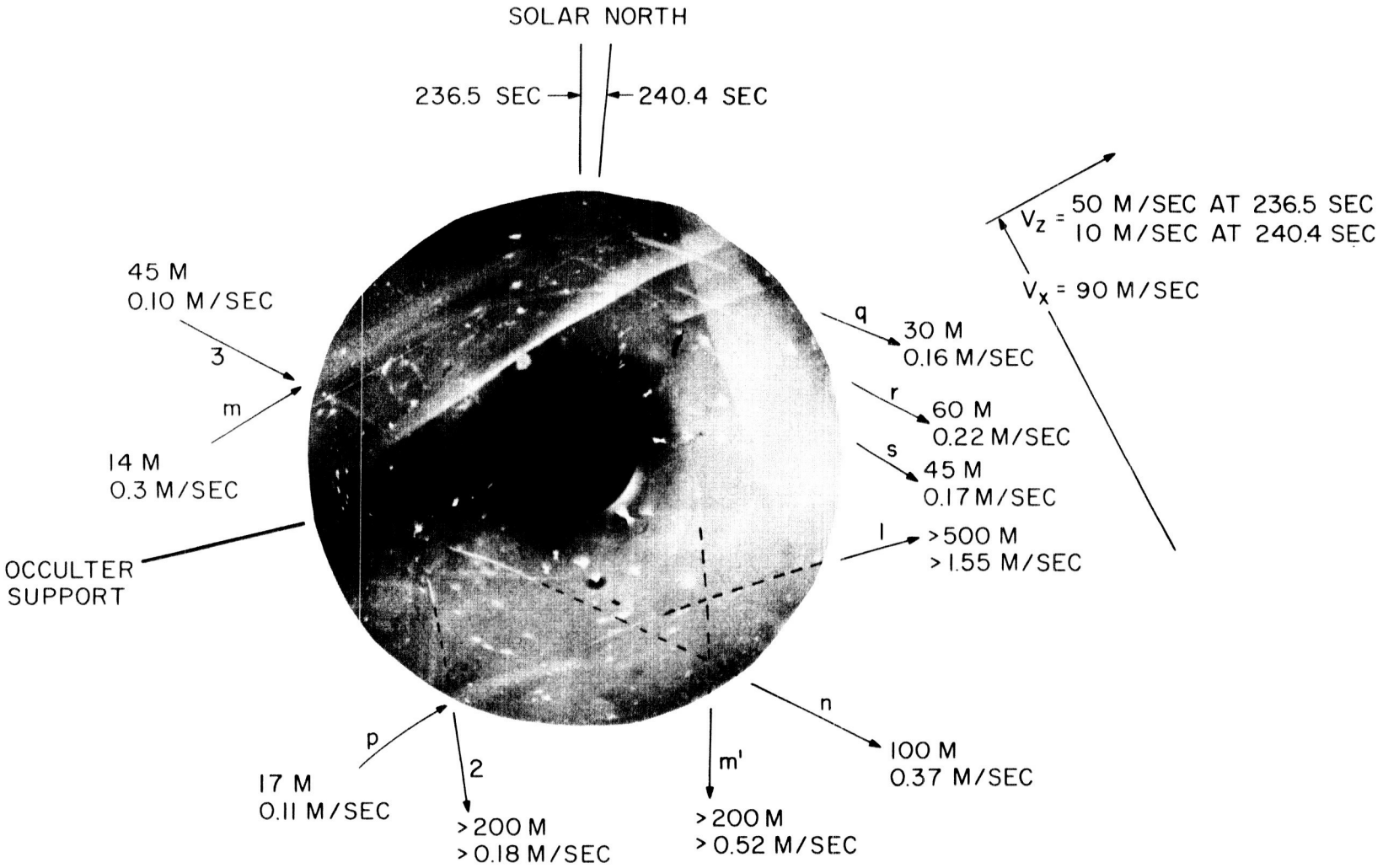

Fig. 6

FRAME #15, 3.8 SEC, 204.2 TO 204.3 KM
AEROBEE NE 3.129 (CORONAGRAPH) 28 JUNE 1963